JOINT EUROPEAN TORUS JET

JET–P(88)53

L-G. Eriksson, T. Hellsten, D.A. Boyd, D.J. Campbell, J.G. Cordey, W. Core, J.P. Christiansen, G.A. Cottrell, J.J. Jacquinot, O.N. Jarvis, S. Kissel, C. Lowry, P. Nielsen, G. Sadler D.F.H. Start, P.R. Thomas, P. van Belle, J.A. Wesson and JET Team

Calculations of Power Deposition and Velocity Distributions During ICRH; A Comparism with Experimental Results

Calculations of Power Deposition and Velocity Distributions During ICRH; A Comparism with Experimental Results

L-G. Eriksson[1], T. Hellsten, D.A. Boyd[2], D.J. Campbell, J.G. Cordey, W. Core, J.P. Christiansen, G.A. Cottrell, J.J. Jacquinot, O.N. Jarvis, S. Kissel, C. Lowry, P. Nielsen, G. Sadler D.F.H. Start, P.R. Thomas, P. van Belle, J.A. Wesson and JET Team*

JET-Joint Undertaking, Culham Science Centre, OX14 3DB, Abingdon, UK

[1]Chalmers University of Technology, S-41296 Gothenburg, Sweden
[2]University of Maryland, College Park, MD 20742, USA.
** See annex of P. Lallia et al, "Plasma Heating in JET",*
(13th EPS Conference on Controlled Fusion and Plasma Physics, Schliersee, Germany (1986)).

Preprint of Paper to be submitted for publication in
Nuclear Fusion Letters

Calculations of Power Deposition and Velocity Distributions During ICRH; A Comparison with Experimental Results

L-G. Eriksson*, T. Hellsten, D.A. Boyd+, D.J. Campbell, J.G. Cordey, W. Core, J.P. Christiansen, G.A. Cottrell, J.J. Jacquinot, O.N. Jarvis, S. Kissel, C. Lowry, P. Nielsen, G. Sadler, D.F.H. Start, P.R. Thomas, P. van Belle and J.A. Wesson

JET Joint Undertaking, Abingdon, Oxon., OX14 3EA, UK
* Chalmers University of Technology, S-41296 Gothenburg, Sweden
+University of Maryland, College Park, MD 20742, USA.

ABSTRACT

A model is presented which permits the self-consistent calculations of the power deposition and velocity distribution of cyclotron resonance heated ions. The model is applied to minority heating of ^{3}He in D-plasmas in the JET experiment. Good agreement is found between calculated and measured values of fusion yield and energy content of ^{3}He ions. The results indicate that the power deposition is adequately described and that the fast ions slow down on electrons by Coulomb collisions. Measurements of the electron heating after the sawtooth crash show that about 50% of the energy content of the fast ions is retained in the centre after a sawtooth crash.

1. INTRODUCTION

During ion cyclotron resonance heating (ICRH) centrally peaked power deposition profiles are expected when the magnetosonic wave is focussed on the magnetic axis. The large wave fields absorbed in the centre of the plasma will create a non-Maxwellian velocity distribution of the heated ions, which may enhance the fusion yield. The velocity distribution also determines the fraction of RF-power transferred to different background plasma species.

For evaluating transport coefficient during ICRH and for the prediction of the behaviour of ICRH in future machines, reliable deposition profiles are

required. Various numerical methods have been developed to calculate the power deposition profile, e.g. ray tracing [1,2] and global wave codes [3,4]. Analysis of the power deposition with global wave codes shows that the power deposition for ion cyclotron heating depends on the toroidal mode number spectrum, the averaged squared parallel velocity of the heated ions and the single pass absorption along the cyclotron resonance [5]. The velocity distribution, which determines the averaged squared parallel velocity, is in its turn determined by the power deposition. Hence, the power deposition and the velocity distribution have to be calculated self- consistently. Self-consistent calculations of the power deposition and velocity distribution of the heated ions have been performed previously by Morishita et al. [6] in plane geometry and for an isotropic plasma. The model presented in this paper takes into account the two-dimensional effects for the wave propagation and the effects of anisotropic velocity distribution.

Measuring the power deposition accurately is difficult. When direct electron heating dominates, one can measure the power deposition inside the q=1 surface by measuring the energy increase of the electrons after sawtooth crashes. However, this method does not give the power deposition when the electron heating occurs through a high energy ion tail; instead, it gives the electron heating profile by the fast ions and this is not necessarily the ICRH power absorption profile.

Due to the difficulties of measuring the power deposition, it is difficult to assess whether or not the models are applicable to the experiment. To assess this question, we instead compare two indirectly measured quantities for minority heating of ^{3}He in D-plasmas: the fusion yield due to (^{3}He, D) reactions and the energy content of the fast ions.

Good agreement is found between the theoretically calculated and experimentally measured values. However, this does not prove the uniqueness of the calculated power deposition.

2. CALCULATIONS

The launched magnetosonic wave can be absorbed either directly or indirectly via mode conversion by various absorption mechanisms, including ion cyclotron absorption, electron Landau damping and electron transit time damping. Linear mode conversion can take place on the high field side of the cyclotron resonance of ^{3}He if the minority concentration is large, or the product of $k_{||} \cdot \bar{v}_{||}$ is small, where $k_{||}$ denote the local parallel wavelength and $\bar{v}_{||}$ the square root of the averaged squared parallel velocity, $\bar{v}_{||}^2 = \langle v_{||}^2 \rangle$. It is also possible to have mode conversion near the plasma boundary at the high field side. For the so-called monopole phasing of the antenna, which peaks the spectrum of toroidal wave numbers at $n_\phi = 0$, the direct electron damping of the magnetosonic wave can be neglected, as can mode conversion near the plasma boundary at the high field side of the cyclotron resonance of deuterium. The two dominant "absorption" mechanisms of the fast wave are then mode conversion close to the cyclotron resonance of ^{3}He and cyclotron absorption. Mode conversion is not a true damping mechanism but takes power away from the magnetosonic wave which is then absorbed elsewhere in the plasma. Only the ion cyclotron absorption is expected to create a high energy tail in the ^{3}He ions and to give an enhancement of the fusion yield above the thermal level. We have neglected the wave power absorbed on the wall and limiters. The total absorbed power then equals the coupled power.

In principle the coupling spectrum, the power deposition and the velocity distribution have all to be calculated self-consistently. For the heating scenario studied here, the single pass absorption is rather weak resulting in cavity resonances. The coupling spectrum will then vary noticeably for small variations of the equilibrium parameters. Since the equilibrium parameters are not known to such an accuracy that a proper

calculation of the coupling spectrum can be made, we calculate the coupling spectrum as if the wave were completely absorbed during its first pass across the plasma. This coupling spectrum represents the averaged coupling spectrum for small variations of the equilibrium parameters. The coupling spectra for single pass absorption is calculated by Fourier decomposition of the antenna current in the toroidal direction, and treating the coupling problem in a plane geometry for each toroidal mode number. Note that complete single pass absorption is only assumed for these antenna coupling calculations.

The part of the power being mode converted is assumed here to heat the electrons and has to be subtracted from the launched power. It is calculated for each toroidal mode number in a plane slab approximation of the absorption layer using the WKB method for the cyclotron absorption and the Budden formula for the mode conversion. For the remaining part of the power, which is absorbed by cyclotron absorption the flux surface averaged power deposition is calculated for each toroidal mode number according to the formula given in Ref.[5].

When the flux surface average power density is known, the velocity distribution of the heated ions can be calculated. This is done by solving a one-dimensional equation for the velocity distribution, f(v), which has been shown to reproduce accurately both the the fusion yield and the ratio of electron heating to ion heating [7]. We have included in the Fokker-Planck equation, a finite energy confinement time of the heated ions of 0.4s, which is a typical value for the confinement time of the bulk plasma. The averaged parallel velocity squared is calculated from this velocity distribution using the following formula [8]

$$\langle v_{||}^2 \rangle = \int \mu_{eff}^2 \, v^2 \, f(v) \, 4\pi \, v^2 \, dv \qquad (1)$$

$$\mu_{eff}^2 = \frac{1 + (v/v^*)^2}{3(1 + (v/v^*)^2 + (v/v^*)^4)} \qquad (2)$$

where $v^* = 0.5v_\gamma$, v_γ represents the velocity above which pitch angle ceases to be important [9]. The choice of v^* has been obtained by fitting $\langle v_{||}^2 \rangle$ calculated from Eq. (1) with that from the BAFIC code [10]. This code solves a time dependent bounce averaged Fokker-Planck equation which describes quasi linear diffusion in a 2-D velocity space due to ICRH and collisions.

After calculating $\langle v_{||}^2 \rangle$ we compare it with the previous one or the initial ansatz. If the deviation is large we go back and recalculate the power deposition for the new velocity distribution and so on. When the deviation is sufficiently small we compute the fusion yield and energy content of the fast ions for the last calculated velocity distribution. The fusion yield is obtained from a model that assumes that the velocity distribution of the D-ions is a Maxwellian [11]. Typical flux surfaced averaged power deposition are shown in Fig. 1 for 9MW coupled RF power and two different minority concentrations, $n_{^3He}/n_e = 0.1$ and 0.01. The magnetic flux surfaces are labelled by a parameter, $s = \sqrt{\psi/\psi(a)}$, where $\psi(a))$ is the poloidal flux function at the plasma edge. The higher concentration gives a larger fraction of the power to mode conversion but also a higher power density in the centre. In Fig.1 we also show $\bar{P}(s)$, the power density integrated over the plasma volume normalized to the total RF-power.

3. COMPARISON WITH EXPERIMENTAL RESULTS

The discharges with ICRH of ^3He in D-plasmas was characterised by temperatures and densities in the ranges $T_e(0) = 5\text{-}8keV$, $T_i = 4\text{-}8keV$, $n_e(0) = 4\text{-}5 \cdot 10^{13} cm^{-3}$, $n_D/n_e = 0.5\text{-}0.85$, $n_{^3He}/n_e = 1\text{-}10\%$. The RF frequency was 33MHz and the antenna was coupled in the so-called toroidal monopole phasing, peaking the toroidal wave number, n_ϕ at 0 such that $\langle n_\phi^2 \rangle = 100$. The magnetic field was chosen such that the cyclotron resonance passed through the magnetic axis.

The fusion yield due to the reaction D + ^{3}He → H + ^{4}He was deduced by measuring the flux of 16 MeV γ-rays from the reaction: D + ^{3}He → γ + ^{5}Li. The cross-section for the two reactions are nearly proportional to each other in the range 0-1 MeV, but the latter is 2.5×10^{-5} smaller. The γ-flux was measured with sodium iodide and bismuth germanate scintillators [12].

Comparison between experimental measurements and calculated values are shown in Fig. 2. The calculations have been made for the experimentally determined values of electron and ion temperatures and densities. The fusion yield is particularly sensitive to Z_{eff}, T_e, T_D. The uncertainties of these quantities are sufficient to explain the difference between measured and calculated values, e.g. an error in Z_{eff} of 20% gives about 25% change in the fusion yield. There is also some uncertainty in the calibration of the fusion yield.

In Fig. 3 we have plotted the fusion yield as a function of s. As the coupled power increases, the fusion yield in the centre decreases. The slope of the fusion yield versus power diminishes when the power density becomes so high that the minority ions are heated up above the maximum cross-section for (^{3}He, D) reactions.

The energy content of the minority ions, W_{fast}, can be obtained by taking the difference between the change in energy, δW_{dia}, based on measurements of the diamagnetic effect and the change in energy, δW_{kin}, based on measuring plasma density and temperature

$$W_{fast} = \frac{2}{3} (\delta W_{dia} - \delta W_{kin}). \qquad (3)$$

W_{kin} is calculated from electron temperature measurements obtained from ECE radiation, electron density from the multi-channel far infrared interferometer and ion temperature from the X-ray crystal spectrometer through the formula

$$W_{kin} = \int T_e\, n_e \left(1 + \frac{T_i(o)}{T_e(o)} \cdot \left(\frac{6 - Z_{eff}}{5} + \frac{Z_{eff} - 1}{30}\right)\right) d^3r \qquad (4)$$

where Z_{eff} is obtained from the visible bremsstrahlung measurement. The density of ^3He is estimated by measuring the increase in the electron line density after ^3He is puffed in. Comparison between measured values and calculated are shown in Fig. 4. For these calculations, we have assumed the impurities to be dominated by carbon.

In another series of discharges the measured and the theoretically computed fusion yield disagreed more, although they were still of the same order of magnitude. However, the agreement for the energy content was good. These discharges were run after pulse discharge cleaning with ^4He. It is possible that the two series of discharges had different compositions of impurities giving rise to different deuterium concentrations.

From Figs. 2 and 4 one finds a threshold of the coupled RF power for tail formation of about 4MW. This threshold is in good agreement with the calculations.

If we assume that the increase in the energy of the electrons after a sawtooth crash is mainly due to the slowing down of fast ions and other mechanisms affecting the energy balance can be neglected, then the energy content of the fast ions can then be obtained by measuring the increase in the local electron energy, $\dot{W}_e(s)$

$$W_{fast}(s) = \dot{W}_e\, t_s/2 \qquad (5)$$

where t_s is the slowing down time for ion-electron collisions [8]. The increase in the electron temperature is measured with the 12-channel polychromator [13].

In Fig. 5 we compare the measured $\dot{W}_e$ and the calculated p_e for a discharge. The calculated power deposition is much more peaked than the measured heating profiles. The reason for this discrepancy can be understood in that the experimentally measured heating profile is due to the heating of the ions after a sawtooth crash. It is also possible that the fast ions are redistributed spatially during sawtoothing. Also, in the calculations we have neglected the finite drift orbits and RF-induced diffusion of the heated ions. All these effects will give a broader heating profile.

We also compare, in Fig.4, the energy contents of the fast ions near the centre obtained by integrating Eq. (5) with the calculated values and those measured according to formula (3). This energy is about 50% lower, implying that about 50% of the fast ions are confined in the centre of the plasma after a sawtooth crash.

4. CONCLUSIONS

The self-consistent calculations of the power deposition and velocity distribution are in good agreement with the experimentally measured fusion yield and energy content of fast ions. The models for calculating the power deposition and velocity distribution has been benchmarked with the LION [4] and BAFIC [10] codes, respectively. The good agreement suggests that the underlying physical assumptions adequately describe the reality. Thus the slowing down of the fast ions on the electrons occurs by Coulomb collisions and the propagation of the waves are described properly.

The calculations indicate that the ^{3}He ions in the centre are heated above the maximum cross-section for fusion reactions. The minor radius of magnetic surface for which the maximum fusion yield occurs increases with increasing power.

The energy content of the heated ions will increase with increasing peaking of the power deposition since the electron temperature is highest in

the centre. Similar agreement can be obtained for different profiles but the power density in the centre will determine the threshold for tail formation. The present agreement between experiment and calculations is a good indication that the calculations of central power density are correct. The discrepancy between measured electron heating profiles after a sawtooth crash can be due to the redistribution of fast ions or the finite orbit effects or RF-induced diffusion of the fast ions. The minor radius of the magnetic surface for which the maximum fusion yield occurs increases with increasing power.

There seems to be a systematic difference between measured and calculated values of the fusion yield. However, this should be put in the perspective that, according to the calculations, the fusion yield in the centre increases by about five orders of magnitude when the RF-power is switched on. Furthermore, the variation in the calculated fusion yield due to the uncertainties in the D and ^{3}He concentrations and ion temperature is larger than the discrepancy between the experimental and the calculated values. The energy content of the fast ions is less sensitive to the D and ^{3}He concentration and depends primarily on the power deposition profile, electron temperature and density.

For the discharges with the highest coupled power, the calculations give a mean energy of the ^{3}He ions in the centre of several MeV. The number and the energy of the heated ions is expected to be comparable to that of α-particles created from fusion reactions during D-T operation in JET. Thus minority heating of ^{3}He will be a good simulation of α-particle heating. By measuring the electron heating inside the q=1 surface after a sawtooth crash, we have found that the energy content of the high energy ions, inside this surface, decreases by about 50% during sawtooth crashes.

ACKNOWLEDGEMENT

We would like to acknowledge the JET team members who have operated the tokamak and the ICRH system and to the members of the diagnostic groups involved in the measurements reported here.

REFERENCES

[1] Brambilla, M., RAYC - A numerical code for the study of ion cyclotron heating of large tokamak plasma. Max-Planck-Institut für Plasmaphysik, Garching, IPP 4/216 (1984).

[2] Koch, R., Bhatnagar, V.B., Messiaen, A.M., van Ester, D., Computer Physics Communication 40 (1986) 1.

[3] Itoh, K., Itoh, S.-I., Fukymama, A., Nucl. Fusion 24 (1984) 13.

[4] Villard, L., Appert, K., Gruber, R., Vaclavik, J., Comp. Phys. Reports 4 (1986) 95.

[5] Hellsten, T., Villard, L., Nucl. Fusion 28 (1988) 285.

[6] Morishita, T., Fukuyama, A., Hamamatsu, K., Itoh, S-I., and Itoh, K., Nucl. Fusion 27 (1987) 1291.

[7] Anderson, D., Core, W., Eriksson, L.-G., Hamnén, H., Hellsten, T., Lisak, M., Nucl. Fusion 27 (1987) 911.

[8] Anderson, D., Eriksson, L.-G., Lisak, M., Plasma Physics and Controlled Fusion 29 (1987) 891.

[9] Stix, T.H., Nucl. Fusion 15 (1975) 737.

[10] Hellsten, T., Appert, K., Core, W., Hamnén, H., Succi, S., Proc. of 12th EPS Conf. on contr. Fus. and Plasma Phys., Budapest (1985), Vol.II, p.124.

[11] Core, W.G.F., Private communications.

[12] Sadler, G., Jarvis, O.N., van Belle, P., Hawkes, N., Syme, B., Proc. of 14th EPS Conf. on Contr. Fus. and Plasma Phys., Madrid (1987), Vol.III, p.1232.

[13] Tubbing, B.J.D., Barbien, E., Campbell, D.J., Hugenholtz, C.A.J. et al., in Contr. Fusion and Plasma Physics, Proc. 12th European Conf., Budapest 1985, Vol.9F-I (1985) p.215.

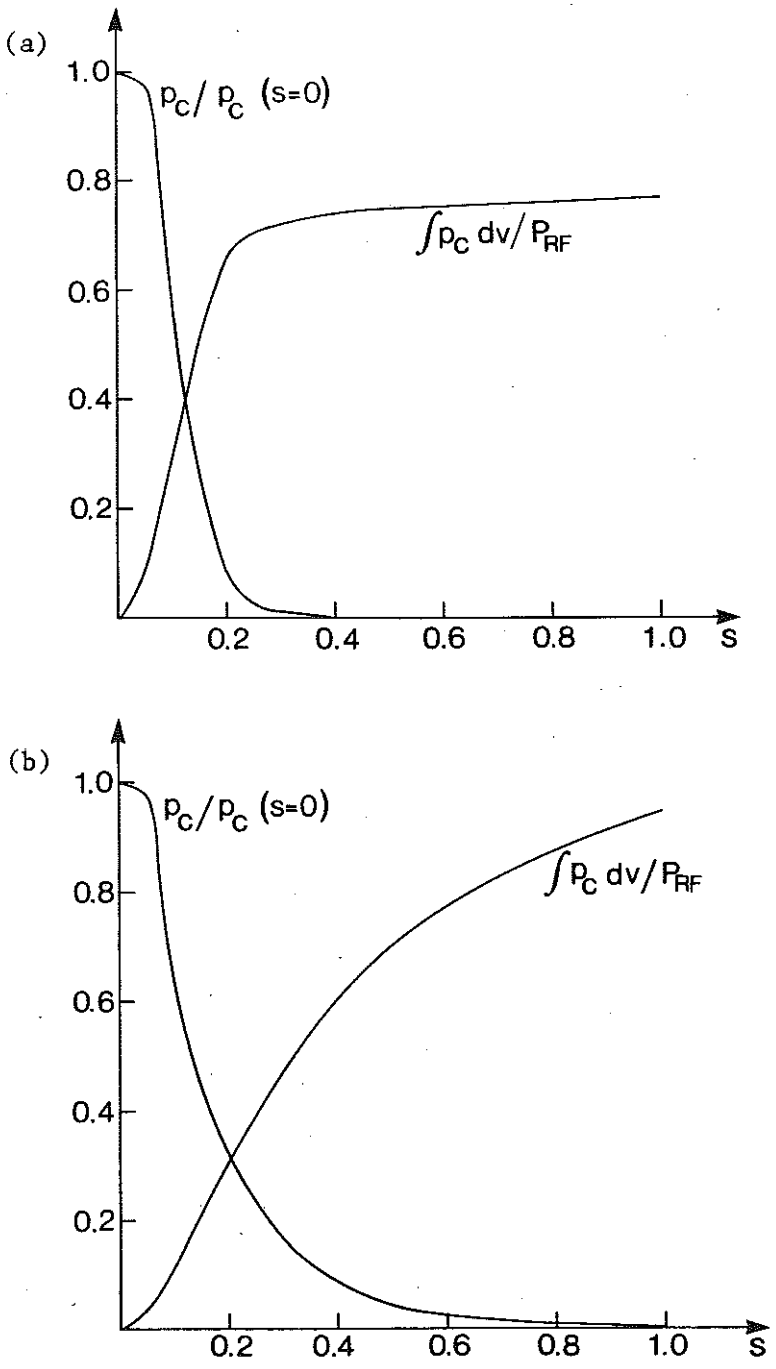

Fig. 1 Power density $p_c(s)$ absorbed by the minority ions through cyclotron damping averaged over a magnetic flux surface and integrated from the magnetic axis to the flux surface s. Calculated for 9MW coupled power, $n_e(o)=4.4\times10^{13}\text{cm}^{-3}$, $Z_{eff}=3.5$, $T_D(o)=5\,\text{keV}$, $T_e(o)=7\,\text{keV}$.

a) $n^3_{He}/n_e=0.01$, $p_c(s=0)=1.8\,\text{W/cm}^3$
b) $n^3_{HE}/n_e=0.10$, $p_c(s=0)=4.5\,\text{W/cm}^3$

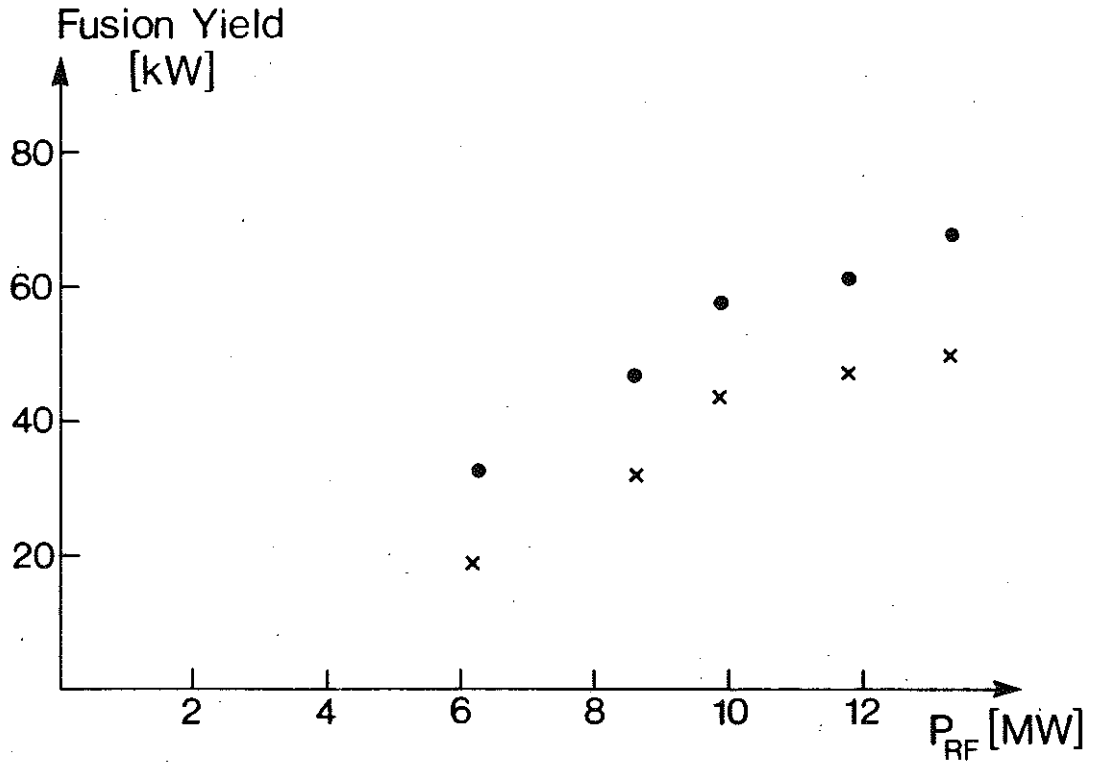

Fig. 2 Fusion yield versus coupled RF-power for various discharges, (.) calculated values, (+) measured values.

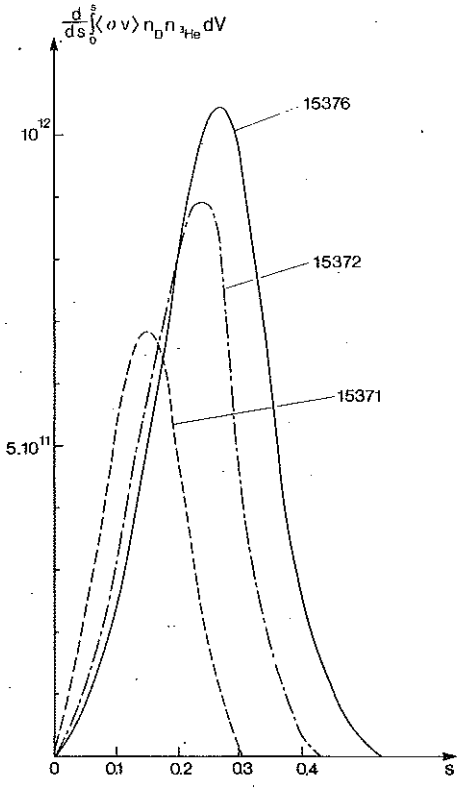

Fig. 3 Fusion yield integrated over a flux surface versus s for three different discharges with coupled RF-power, 6.1 MW, 8.3 MW and 13.2 MW.

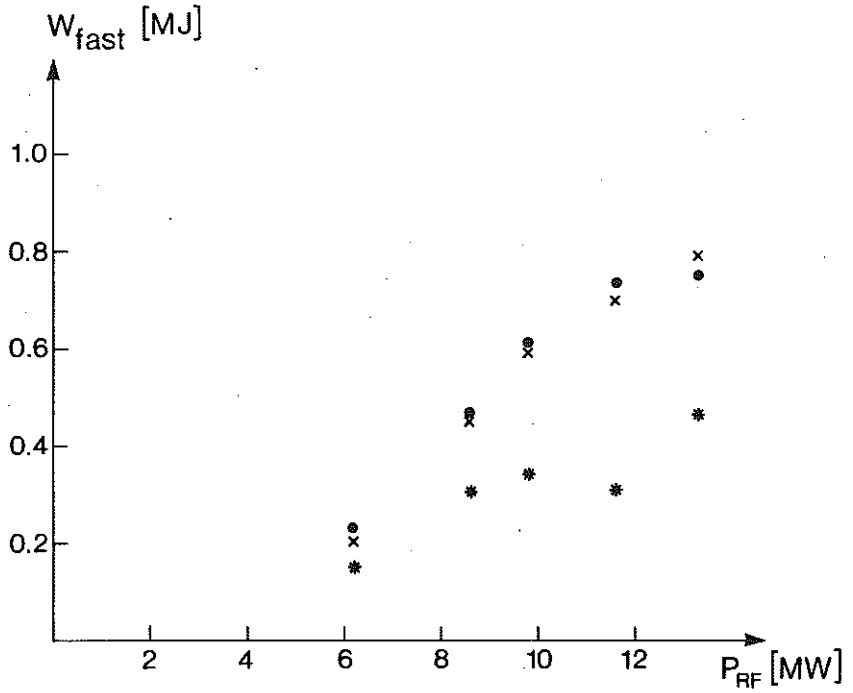

Fig. 4 Energy content versus coupled RF-power, (.) calculated values, (+) measured values and (*) energy content of fast ions after a sawtooth crash.

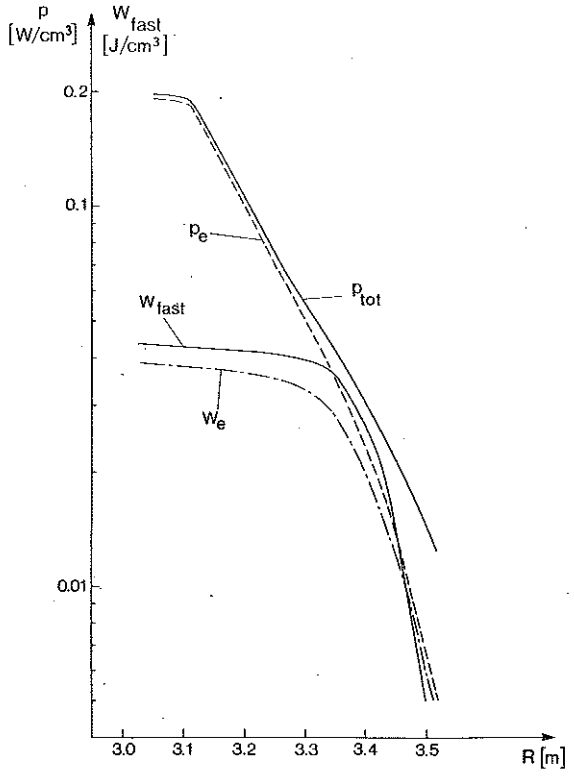

Fig. 5 Calculated flux surface averaged power density and power transfer to electrons for two discharges with coupled power of 6.15MW and 13.2MW respectively. Measured electron heating, P_{em}, and $W_{fast}(s)$ after a sawtooth crash.